Frontiers of Physics
https://doi.org/10.1007/s11467-019-0895-2
Front. Phys.
14(5), 53601 (2019)

RESEARCH ARTICLE

Possible phase transition of anisotropic frustrated Heisenberg model at finite temperature

Ai-Yuan Hu†, Lin Wen‡, Guo-Pin Qin, Zhi-Min Wu, Peng Yu, Yu-Ting Cui

College of Physics and Electronic Engineering, Chongqing Normal University, Chongqing 401331, China
Corresponding authors. E-mail: †huaiyuanhuyuanai@126.com, ‡wlqx@cqnu.edu.cn
Received May 9, 2018; accepted January 16, 2019

The frustrated spin-1/2 J_{1a}–J_{1b}–J_2 antiferromagnet with anisotropy on the two-dimensional square lattice was investigated, where the parameters J_{1a} and J_{1b} represent the nearest neighbor exchanges and along the x and y directions, respectively. J_2 represents the next-nearest neighbor exchange. The anisotropy includes the spatial and exchange anisotropies. Using the double-time Green's function method, the effects of the interplay of exchanges and anisotropy on the possible phase transition of the Néel state and stripe state were discussed. Our results indicated that, in the case of anisotropic parameter $0 \leq \eta < 1$, the Néel and stripe states can exist and have the same critical temperature as long as $J_2 = J_{1b}/2$. Under such parameters, a first-order phase transformation between the Néel and stripe states can occur below the critical point. For $J_2 \neq J_{1b}/2$, our results indicate that the Néel and stripe states can also exist, while their critical temperatures differ. When $J_2 > J_{1b}/2$, a first-order phase transformation between the two states may also occur. However, for $J_2 < J_{1b}/2$, the Néel state is always more stable than the stripe state.

Keywords frustrated Heisenberg model, quantum phase transition, magnetic anisotropy, antiferromagnetics

1 Introduction

In recent years, the study of frustrated spin model has become very active on two-dimensional (2D) square lattice with nearest-neighbor (NN) and next-nearest-neighbor (NNN) antiferromagnetic exchange interactions (known as J_1–J_2 model) [1–12]. The frustration is caused by the mutual competition between J_1 and J_2, which can trigger a rich phase diagram [1]. Therefore, in the past, this model had been widely investigated by means of various theoretical methods (see, e.g., [12], and references). It was well known that the ground state usually showed two possible antiferromagnetic states. One is called Néel state (NS), and the other is called stripe state (SS). The NS was characterized by an antiparallel alignment of NN spins with a corresponding magnetic wave vector $Q_{\rm NS}(\pi,\pi)$, see Fig. 1. The SS was twofold degenerated and the corresponding magnetic wave vectors were $Q^1_{\rm SS}(\pi,0)$ and $Q^2_{\rm SS}(0,\pi)$, which were characterized by the fact that the NN spins take a parallel orientation in the vertical (horizontal) direction and an antiparallel orientation in the horizontal (vertical) direction, respectively, see Fig. 1. Investigations indicated that the system was an NS for $\alpha = J_2/J_1 \lesssim 0.38$, and for $\alpha \gtrsim 0.6$ it turned to be an SS. When $0.38 \lesssim \alpha \lesssim 0.6$, it was a nonmagnetic quantum phase [1–12]. At zero temperature, the key question is to understand the nature of the non-magnetic phase in the intermediate J_2/J_1 regime [3, 13].

For finite temperature, there is no long-range order for isotropic 2D model [14]. Usually, an anisotropy is considered. This is because that an anisotropy, no matter how is faint, will cause a long-range order at finite temperature. Therefore, at finite temperature, the investigative emphasis is to discuss the effect of the anisotropy on the phase diagram. For example, Viana *et al.* studied the phase diagram of a exchange anisotropic J_1–J_2 model at finite temperature [2]. Their results indicated that between the paramagnetic and stripe phases the system underwent a first-order transition at low temperature and a second-order transition at high temperature. The investigation of Roscilde *et al.* showed that when an Ising type exchange anisotropy was induced, there would be Chandra–Coleman–Larkin transition and Berezinskii–Kosterlitz–Thouless transition [9]. These investigations indicated that the anisotropy played an important role.

A generalization of the J_1–J_2 Heisenberg antiferromagnetic model on a square lattice was introduced by Nersesyan and Tsvelik [15], the so-called J_{1a}–J_{1b}–J_2 model [16, 17]. It possesses more degrees of freedom to tune the fluctuation of system compared to the J_1–J_2 model, since the NN exchange interactions J_{1a} and J_{1b} along the x and y directions in this model are of different strengths. This feature leads naturally to an increased sensitivity of the

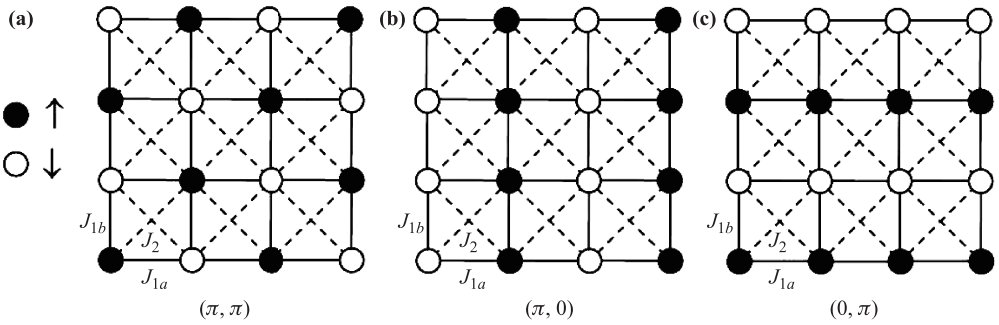

Fig. 1 Spin configurations of the Néel and stripe states. **(a)** the Néel state (π, π), **(b)** the stripe state $(\pi, 0)$, and **(c)** the stripe state $(0, \pi)$. The stripe state is twofold degenerated. The solid and empty circles represent the up-spins and down-spins, respectively.

underlying Hamiltonian to the presence of small perturbations.

Extensive band structure calculations for the vanadium phosphate compounds $Pb_2VO(PO_4)_2$, $SrZnVO(PO_4)_2$, $BaZnVO(PO_4)_2$, $BaCdVO(PO_4)_2$ had shown four different exchange couplings: J_{1a} and J_{1b} between the NN and J_2 and J_2' between NNN [18]. For example, $J_{1b}/J_{1a} \approx 0.7$ and $J_2'/J_2 \approx 0.4$ were obtained for $SrZnVO(PO_4)_2$. A possible candidate for J_{1a}–J_{1b}–J_2 model might be the compound $(NO)Cu(NO_3)_3$ though band-structure calculations showed a uniform spin chain model with different types of anisotropy and weak interchain couplings [19, 20].

Our primary purpose of this work is to study the phase transition of the J_{1a}–J_{1b}–J_2 model at finite temperature by using the double-time Green's function (DTGF) method. Our results indicate that at $0 \leq \eta < 1$ (where η is the anisotropic parameter.) both NS and SS can exist and have the same critical temperature as long as $J_2 = J_{1b}/2$. When $J_2 \neq J_1/2$, these two states may also exist, but their critical temperatures differ. The calculated free energies for these two cases show that a first-order phase transformation between NS and SS below critical points can occur. Which of the states is more stable, it will depend on the spatiality and exchange anisotropies of the system.

This paper is organized as follows. In Section 2, we introduce the theoretical model, and present the formulism of Green's function to derive the self-consistent equation for evaluation of magnetizations. In Section 3, the numerical results are presented and discussed. Section 4 is our concluding remarks.

2 Model and method

The Hamiltonian of J_{1a}–J_{1b}–J_2 model can be written as

$$\begin{aligned} H = {} & J_{1a} \sum_{\langle i,j \rangle} \left[\eta(S_i^x S_j^x + S_i^y S_j^y) + S_i^z S_j^z\right] \\ & + J_{1b} \sum_{\langle i,j \rangle} \left[\eta(S_i^x S_j^x + S_i^y S_j^y) + S_i^z S_j^z\right] \\ & + J_2 \sum_{[i,j]} \left[\eta(S_i^x S_j^x + S_i^y S_j^y) + S_i^z S_j^z\right], \end{aligned} \tag{1}$$

where S_i^x, S_i^y and S_i^z represent the three components of the spin-S operator for a spin at site i. The sums $\langle i, j \rangle$ and $[i, j]$ run over the NN and NNN lattice sites, respectively. η denotes the anisotropic parameter with $0 \leq \eta < 1$. Spin quantum number is $S = 1/2$ and the lattice is the 2D square lattice. We fix $J_{1a} = 1$ and change other parameters in computation.

For the sake of convenience, we let Boltzmann constant $k_B = 1$. The sublattice magnetization is defined as $m = \langle S^z \rangle$. where $\langle S^z \rangle$ is the assembly statistical average of spin operator S^z.

In this paper, we will use the DTGF method to investigate the phase transition properties of the system. The DTGF method used in Refs. [21] and [22] is known as the standard method in the study of magnetic systems. In this method one obtains a nonlinear differential equation in which the higher-order Green's functions are coupled with the lower-order ones. Each of the higher-order Green's functions is again written down in the form of a nonlinear equation and so on. To obtain tractable solutions, decoupling procedures have been invoked to terminate the hierarchy of Green's functions generated by the equations of motion. Many results for the thermodynamic properties have been obtained in a frame of the simplest decoupling, i.e., the random phase approximation decoupling [21, 22]. The decoupling provides a simple enough way for giving results in good agreement with other approaches and experiments in a wide range of temperatures and magnetic fields [23, 24].

The Green's function (GF) is defined as [21, 22]

$$G_{ij}^{+-} = \langle\langle S_i^+; \mathrm{e}^{uS_j^z} S_j^- \rangle\rangle. \tag{2}$$

Here, u is a parameter [22]. After solving the GF by means of the method of equations of motion, u will be ultimately set as zero to give the expression of magnetization [22]. We derive the equation of motion of the GF by a standard procedure [21, 22]. In the course of derivation, the higher order GFs have to be decoupled. In this paper, we apply random phase approximation [21, 22] to decouple the higher order GFs in the equations of motion,

$$\langle\langle S_l^z S_i^+; \mathrm{e}^{uS_j^z} S_j^- \rangle\rangle = \langle S_l^z \rangle \langle\langle S_i^+; \mathrm{e}^{uS_j^z} S_j^- \rangle\rangle; \quad l \neq i. \tag{3}$$

After decoupling of the higher order GFs and standard procedure [21, 22], we obtain

$$\frac{2}{N}\sum_k \langle e^{uS_i^z} S_i^- S_i^+\rangle(k) = \theta(u)\phi_F, \quad F = \mathrm{NS}, \mathrm{SS}, \tag{4}$$

where the summation of wave vector k runs over the first Brillouin zone. N is the number of lattice sites and

$$\theta(u) = \langle [S_i^+, e^{uS_j^z} S_j^-]\rangle. \tag{5}$$

For $u = 0$, $\theta(u) = 2m$. Using Eqs. (4) and (5), we obtain

$$\phi_F = \frac{2}{N}\sum_k \frac{E_{1F}}{2\sqrt{E_{1F}^2 - E_{2F}^2}} \coth\frac{\sqrt{E_{1F}^2 - E_{2F}^2}}{2T} - \frac{1}{2}. \tag{6}$$

Here for the NS,

$$\begin{aligned} E_{1\mathrm{NS}} &= 4J_2 m(\eta\cos k_x \cos k_y - 1) + 2m(J_{1a} + J_{1b}),\\ E_{2\mathrm{NS}} &= 2\eta m(J_{1a}\cos k_x + J_{1b}\cos k_y), \end{aligned} \tag{7}$$

and for the SS,

$$\begin{aligned} E_{1\mathrm{SS}} &= 2J_{1b} m(\eta\cos k_y - 1) + 2m(J_{1a} + 2J_2),\\ E_{2\mathrm{SS}} &= 2\eta m(J_{1a}\cos k_x + 2J_2\cos k_x \cos k_y). \end{aligned} \tag{8}$$

Using Eqs. (5), (6) and the relation $\langle S_i^- S_i^+\rangle = S(S+1) - \langle S_i^z\rangle - \langle (S_i^z)^2\rangle$, the sublattice magnetization is expressed by following formula [21, 22]

$$m_F = \frac{(\phi_F + 1 + S)\phi_F^{2S+1} - (\phi_F - S)(\phi_F + 1)^{2S+1}}{(\phi_F + 1)^{2S+1} - \phi_F^{2S+1}}. \tag{9}$$

The Néel points of the two configurations are expressed by

$$\frac{k_B T_{\mathrm{N,NS}}}{S(S+1)} = \frac{m}{3}\left(\frac{2}{N}\sum_k \frac{E_{1\mathrm{NS}}}{E_{1\mathrm{NS}}^2 - E_{2\mathrm{NS}}^2}\right)^{-1}, \tag{10}$$

and

$$\frac{k_B T_{\mathrm{N,SS}}}{S(S+1)} = \frac{m}{3}\left(\frac{2}{N}\sum_k \frac{E_{1\mathrm{SS}}}{E_{1\mathrm{SS}}^2 - E_{2\mathrm{SS}}^2}\right)^{-1}, \tag{11}$$

respectively.

3 Results and discussion

At zero temperature, our numerical calculations show that the phase diagram of the system is a classical result based on the DTGF. This case will not be discussed here. In this paper, we focus on the properties at finite temperature. Therefore, when we say zero temperature, we actually mean that temperature is very close to zero, which is denoted by $T = 0^+$.

3.1 Magnetic properties

In this section, the basic magnetic properties of the system under various parameters are presented and discussed.

Figure 2 plots the results of magnetization m as a function of temperature T at different parameter values. Figure 2(a) shows the case of $\eta = 0.5$ and $J_{1b} = 0.8$. It is seen that it is NS configuration at $J_2 \le 0.4$. For $J_2 \ge 0.4$, it is SS configuration. As $J_2 = 0$, it is an ordinary 2D antiferromagnetic model. There is no competition to cause frustration. As J_2 increases from zero, the competition between J_{1b}/J_{1a} and J_2/J_{1a} emerges. Since we have fixed $J_{1a} = 1$ in computation, this competition is actually between J_{1b} and J_2. When the value of J_{1b} is fixed, the frustration becomes stronger with the increase of J_2 value. This leads to that $T_{\mathrm{N,NS}}$ and m_{NS} decrease with the increase of J_2. At $J_2 = 0.4$, the frustration reaches maximum. Therefore, as J_2 rises from 0.4, the role of J_2 becomes more important and the frustration becomes comparatively weaker. It leads to that $T_{\mathrm{N,SS}}$ and m_{SS} increase with increasing J_2 value.

Figure 2(a) indicates that the NS and SS have the same order-disorder transition point at $J_2 = 0.4$. It reflects that both configurations can coexist. Since the value of J_2 is exactly equal to $J_{1b}/2$, it is necessary to see whether at $J_2 = J_{1b}/2$ this conclusion is true for any other η and J_{1b} values. We change J_{1b} values and fix $\eta = 0.5$ at $J_2 = J_{1b}/2$, and the results are shown in Fig. 2(b). It is seen that, as J_{1b} takes value from 0.1 to 1, the critical temperatures of the two states are always equal. It indicates that this conclusion holds for different J_{1b} values at $J_2 = J_{1b}/2$. As $J_{1b} = 0$ and $J_2 = 0$, both NS and SS recover an ordinary one-dimensional anisotropic Heisenberg antiferromagnetic model. In this case, only J_{1a} plays a role. When J_{1b} increases from 0, under the condition of $J_2 = J_{1b}/2$, the role of J_{1a} will gradually become weaker, see Fig. 2(b). However, for $J_{1b} = 0.1$, numerical results indicate that the magnetization curves of the two states are the same,

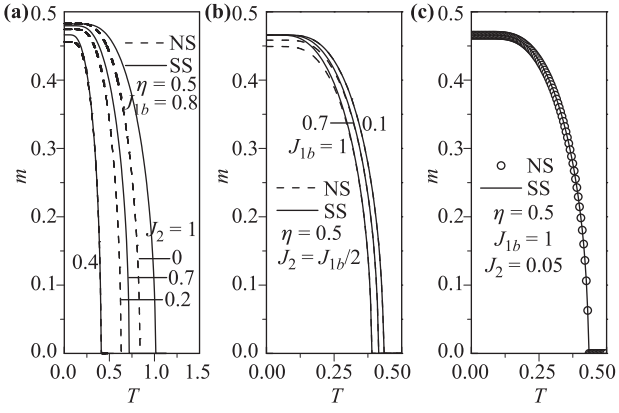

Fig. 2 The sublattice magnetization m as a function of temperature T for various parameters. **(a)** $\eta = 0.5$, $J_{1b} = 0.8$ and various J_2 values. **(b)** $\eta = 0.5$, $J_2 = J_{1b}/2$ and various J_{1b} values. **(c)** It is the case of $J_{1b} = 0.1$ in (b). It is seen that the two curves are identical.

see Fig. 2(c). It reflects that the role of J_{1a} is predominant for small J_{1b} values.

In Fig. 3, $J_{1b} = 0.8$ is fixed and the η varies. It is seen that the two states have the same critical temperature at $0 \leq \eta < 1$ as long as $J_2 = J_{1b}/2$, see Fig. 3(a). The magnetization curves of NS and SS are the same at $\eta = 0$, see Fig. 3(b). This is because that both NS and SS recover an ordinary two-dimensional Ising model. In this case, there are longitudinal but no transverse magnetic correlations between spins. Therefore, as $T \to 0$, the sublattice magnetization becomes fully saturated, i.e., $m(0^+) = 0.5$. Figure 3(a) demonstrates two features as the η value decreases from large to small. One is that both $m_{\rm NS}(0^+)$ and $m_{\rm SS}(0^+)$ increase until full saturation. The other is that the relative difference between $m_{\rm NS}(0^+)$ and $m_{\rm SS}(0^+)$ decreases. Both features are ascribed to the weaker transverse quantum fluctuation for stronger anisotropy. In combination of Figs. 2(b) and 3(a), it is drawn that at $0 \leq \eta < 1$ the two states always have the same critical temperature as long as $J_2 = J_{1b}/2$.

Figure 4 plots the critical temperature as a function of J_2 at different parameters. When $J_{1b} = 0$ and $J_2 = 0$, as mentioned above, both NS and SS recover an ordinary one-dimensional exchange anisotropic Heisenberg antiferromagnetic model. As a consequence, they have the same critical temperature. For NS, as J_{1b} increases from 0, the competition between J_{1b} and J_2 becomes weaker, the frustration of the system also becomes weaker, which leads to rise of the $T_{\rm N,NS}$. SS is just a contrary case, i.e., the $T_{\rm N,SS}$ decreases with increasing J_{1b}. Due to these two reasons, the cross point of the critical temperature curves of the two states shifts rightwards with increasing J_{1b}, see Fig. 4(a). This is actually caused by the competition between J_{1b} and J_2.

Figure 4(b) presents the enlargement of Fig. 4(a) when J_2 is in the vicinity of 0.4 for $J_{1b} = 0.8$. In this panel, the two lines divide the figure into four regions. The upper region, marked by "P", means that the system is in paramagnetic state. The left and right regions are that

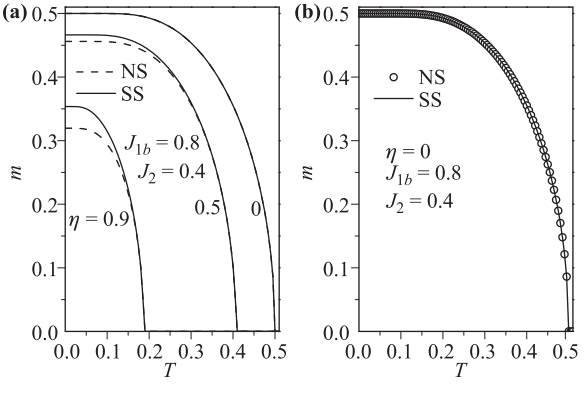

Fig. 3 **(a)** The sublattice magnetization m as a function of temperature T at $J_{1b} = 0.8$ and J_2=0.4 when $\eta = 0$, 0.5, 0.9. **(b)** It is the case of $\eta = 0$ in (a). It is seen that the two curves are identical.

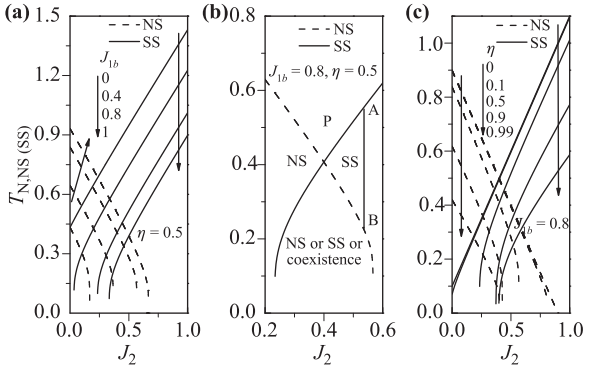

Fig. 4 **(a)** The critical temperature $T_{\rm N,NS(SS)}$ as a function of J_2 for $\eta = 0.5$ when $J_{1b} = 0$, 0.4, 0.8, 1. The left and right arrows represent the J_{1b} from smaller to larger values for NS and SS, respectively. **(b)** The enlargement of the region of J_2 in the vicinity of $J_2 = 0.4$ when $J_{1b} = 0.8$ and $\eta = 0.5$. **(c)** The critical temperature $T_{\rm N,NS(SS)}$ as a function of J_2 for $J_{1b} = 0.8$ when the η increases from 0 to 0.99. The left and right arrows represent the η from smaller to larger for NS and SS, respectively.

the system is in NS and SS configurations, respectively. The lower region can be the coexistence of NS and SS.

Figure 4(c) plots the critical temperature as a function of J_2 for different η values when $J_{1b} = 0.8$. It is seen that the critical temperature increases with the decrease of η. The reason is that the anisotropy suppresses the fluctuation of the system. It leads to that the critical temperature rises. Therefore, the slopes of the critical temperatures of the two states become slower and slower with increasing η, see Fig. 4(c). It leads to the drop of the cross point of the critical temperature between NS and SS. Accordingly, the temperature corresponding to the cross point decreases with the increase of η. As the η value is close to 1, the crossing area disappears. One obtains from Fig. 4 that at $J_{1b} > 0$ and $0 \leq \eta < 1$ the two states always have the same critical temperature as long as $J_2 = J_{1b}/2$.

We have known from the discussion above that both configurations can coexist at $J_2 = J_{1b}/2$ and $J_2 \neq J_{1b}/2$ when $0 \leq \eta < 1$. One may ask which one is more stable. In the following, we manage to answer this question. The two configurations are different from each other, and so are their entropies at a fixed temperature. Therefore, the internal energy cannot be used to determine which one is more stable at each temperature. Under the same volume and temperature, the state with lower free energy is more stable.

The free energy can be evaluated numerically by means of the internal energy via $F(T) = E(0) - T\int_0^T \frac{E(T')-E(0)}{T'^2}{\rm d}T'$, where $E(T)$ represents the internal energy of the system, which is defined as the thermostatistical average of Hamiltonian, $E = \frac{\langle H \rangle}{N}$ [22]. Computing internal energy involves the calculation of the transverse $(\sum_{i,j}\langle S_i^+ S_j^- \rangle)$ and longitudinal $(\sum_{i,j}\langle S_i^z S_j^z \rangle)$ correlation functions. We do not present the lengthy derivation here.

Please refer to Ref. [25].

3.2 Possible phase transition at $J_2 = J_{1b}/2$

In this section, the free energies of NS and SS at $J_2 = J_{1b}/2$ are presented at various parameters, respectively. Since the critical temperatures of the two states equal at $J_2 = J_{1b}/2$, their critical temperatures are uniformly described by T_N.

Figure 5 plots the internal energy $E(T)$ and free energy $F(T)$ as a function of temperature for different J_{1b} values when $\eta = 0.9$. The $E(T)$ increases with temperature as it should be. The $F(T)$ decreases monotonically with temperature. As J_{1b} increases from 0.001 to 0.038, the $F(T)$ curves of NS and SS are identical, i.e., the difference between their free energies is negligible, see Figs. 5(a) and (b). It means that the system can be either the NS or SS, or coexistence of them. For convenience, we denote $J_{1b}^c = 0.038$. As J_{1b} increases from J_{1b}^c, the free energy curves of the two states begin to separate, and $F_{\rm NS}(T) < F_{\rm SS}(T)$, see Fig. 5(c). In this case, NS is more stable in the range of $T \leq T_{\rm N}$. Meanwhile, the free energy of SS with increasing temperature drops faster than of NS. Therefore, when J_{1b} further increases, the free energy curves of the two states cross at an intermediate temperature point, see Fig. 5(d). Therefore, below the temperature of this cross point, $F_{\rm NS}(T) < F_{\rm SS}(T)$. It means that NS is more stable. Above the temperature of this cross point, $F_{\rm NS}(T) > F_{\rm SS}(T)$, so that SS is more stable. At this cross point, there can occur a NS–SS phase transition. Note that, at the cross point, although the free energies of the NS and SS are the same, their internal energies differ, see Fig. 5(d). Subsequently, the specific heat at this cross point is discontinuous (not shown). Therefore, it is a first-order transition.

Figure 6 plots $E(T)$ and $F(T)$ as a function of temperature for different η values when $J_{1b} = 0.9$. Similar to Fig. 5(b), for a fixed J_{1b}, there is an upper limit η^c. When $0 \leq \eta \leq \eta^c$, the difference of the free energy between NS and SS is negligible, i.e., $F_{\rm NS}(T) = F_{\rm SS}(T)$, see Figs. 6(a) and (b). When η increases from η^c, $F_{\rm NS}(T) < F_{\rm SS}(T)$, see Fig. 6(c). As η continues increasing, the free energy curves of the two states cross, see Fig. 6(d). Therefore, its results are similar to Fig. 5. However, it can be found from Figs. 5(d) and 6(d) that, when the values of η and/or J_{1b} increase, it can lead to that the free energy curves of SS with increasing temperature drops faster than of NS. Therefore, when η and/or J_{1b} takes a certain value, the $F_{\rm NS}(T)$ value may be greater than $F_{\rm SS}(T)$. To be explicit, Fig. 7 presents free energy as a function of temperature for $J_{1b} = 0.95$ when $\eta = 0.9$, 0.999. It is seen that the free energy curves of SS with increasing η drops faster than of NS. When $\eta = 0.999$, $F_{\rm NS}(T) > F_{\rm SS}(T)$, see Fig. 7(b). In this case, it means that SS is more stable.

In Figs. 5–7, we only calculate the free energies of the NS and SS as a function of temperature at fixed J_{1b} and η when $J_2 = J_{1b}/2$, one may expect to obtain a number of transitions between NS and SS. Therefore, in Fig. 8, we present a comprehensive recognition of the effect of parameters J_{1b} and η on the free energies of the two states below the $T_{\rm N}$. All possible relationships are presented in Fig. 8(a). There are four regions in Fig. 8(a). Some of them are very narrow. Then we show a enlargement of the region in Fig. 8(b).

In region I, the difference of the free energy between the two states is negligible. So it is denoted as $F_{\rm NS} = F_{\rm SS}$. The examples are the curves in Figs. 5(a, b) and Figs. 6(a, b). It indicates that in this region the system may be either the NS or SS, or coexistence of them.

In region II, the free energy of NS is always less than

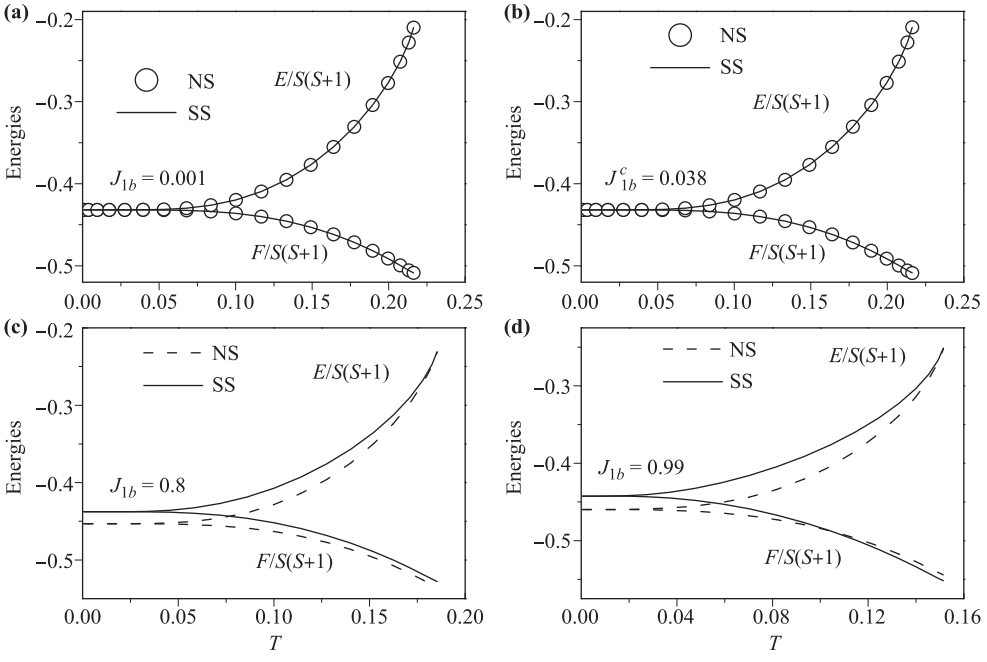

Fig. 5 The internal energies $E(T)$ (ascending lines) and free energies $F(T)$ (descending lines) as a function of temperature T for various J_{1b} values when $\eta = 0.9$. **(a)** $J_{1b} = 0.001$, **(b)** $J_{1b} = J_{1b}^c = 0.038$, **(c)** $J_{1b} = 0.8$, and **(d)** $J_{1b} = 0.99$.

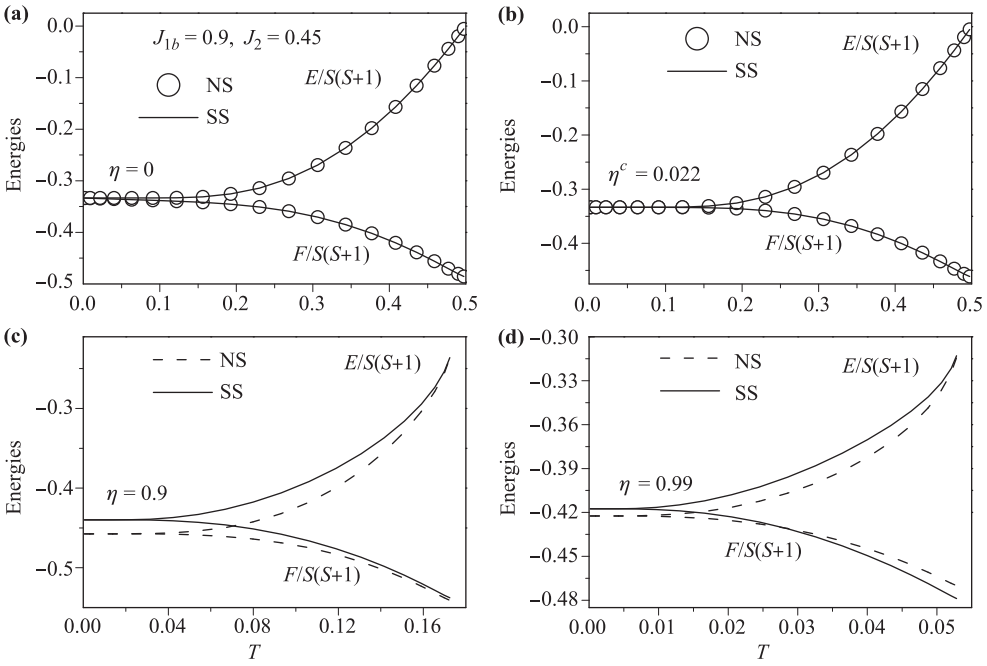

Fig. 6 The internal energies $E(T)$ (ascending lines) and free energies $F(T)$ (descending lines) as a function of temperature T for various η values when $J_{1b} = 0.9$ and $J_2 = 0.45$. **(a)** $\eta = 0$, **(b)** $\eta = \eta^c = 0.022$, **(c)** $\eta = 0.9$, and **(d)** $\eta = 0.99$.

SS. The examples are the curves in Fig. 5(c) and Fig. 6(c). This region is denoted as $F_{\rm NS} < F_{\rm SS}$. It shows that in region II NS is more stable.

In region III, the $F(T)$ curves of the two states cross. The examples are curves in Figs. 5(d), 6(d), and 7(a). When the temperature closes to zero, $F_{\rm NS}(0^+) < F_{\rm SS}(0^+)$. However, when the temperature approaches to the T_N, $F_{\rm NS}(T) > F_{\rm SS}(T)$. Therefore, as temperature is near zero, the state of the system should be NS, and as temperature rises, it is possible to occur a first-order phase transformation from the NS to SS at the cross point below the $T_{\rm N}$.

In region IV, the free energy of $F_{\rm NS}$ is always larger than $F_{\rm SS}$. It shows that in region IV SS is more stable. The example is the curves in Fig. 7(b).

In Fig. 8, two points need to be stressed. One is that in region I, the free energies of NS and SS are very close to each other and one cannot tell which one is more stable. However, as $J_{1b}(\eta)$ increases from $J^c_{1b}(\eta^c)$, region I gradually transits to region II. The other is that for region IV, its boundary seems to be $\eta = 0.9999$. This is because we only compute the case of $\eta = 0.9999$, see Fig. 8(b). Actually, its boundary is $\eta \to 1$. For $\eta = 1$, the system is a two-dimensional isotropic antiferromagnetic model. According to the well-known Mermin–Wagner theorem [14], there is no long-range order at finite temperature for 2D isotropic antiferromagnetic system. Therefore, this case shall be not discussed at finite temperature.

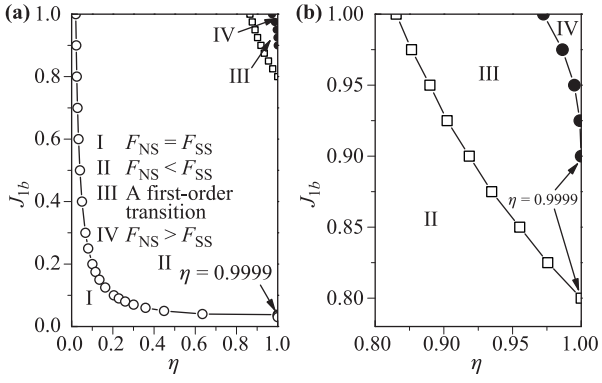

Fig. 8 **(a)** The comparison of the free energies of the two states below the $T_{\rm N}$ in the η and J_{1b} parameter space. There are four regions. **(b)** The enlargement of the region $0.85 \le \eta < 1$ and $0.78 \le J_{1b} \le 1$ in (a). In region I, $F_{\rm NS} = F_{\rm SS}$. In region II, $F_{\rm NS} < F_{\rm SS}$. In region III, the free energy curves of the two states cross. In region IV, $F_{\rm NS} > F_{\rm SS}$.

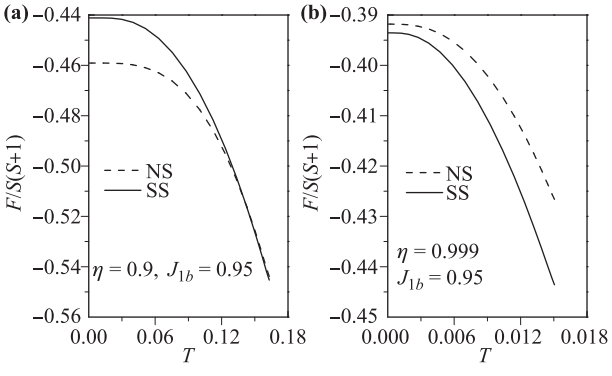

Fig. 7 The free energy $F(T)$ as a function of the temperature T for different η values when $J_{1b} = 0.95$ and $J_2 = 0.475$. **(a)** $\eta = 0.9$, **(b)** $\eta = 0.999$.

3.3 Possible phase transition at $J_2 \neq J_{1b}/2$

When the J_2 value is apart from $J_{1b}/2$, the NS and SS can also coexist, as revealed by Fig. 4(b). In this case, the system should also be in the state with the lower free energy at any temperature. If the $F(T)$ curves of the NS and

SS have cross point, there may occur a phase transition between them. Figure 9 plots the free energy as a function of temperature for different J_2 values when $\eta = 0.5$ and $J_{1b} = 0.8$. It is seen from Figs. 9(a) and (b) that, as the value of J_2 increases from 0.25 to 0.39, the difference of the free energies between the two states gradually becomes small, especially near critical temperature, see the curves in Fig. 9(b). It seems to tell us when J_2 approaches 0.4, the free energy curves of the two states may cross. Nevertheless, numerical calculations indicate that at $J_2 \to 0.4$, $F_{\rm NS}(T) < F_{\rm SS}(T)$. This case is not shown here. In fact, Fig. 8(a) clearly shows $F_{\rm NS}(T) < F_{\rm SS}(T)$ at $\eta = 0.5$ and $J_2 = 0.4$. Therefore, $F_{\rm NS}(T)$ is always less than $F_{\rm SS}(T)$ at $J_2 < 0.4$. This means that in this case NS is more stable. For the case of $J_2 > 0.4$, one should distinguish three cases. (1) $0.4 < J_2 < 0.4088$, $F_{\rm NS}(T)$ is still less than $F_{\rm SS}(T)$, see the curves with $J_2 = 0.401$ in Fig. 9(c). In this case, NS is more stable. At $J_2 = 0.4088$, when $T \to 0$, the free energies of the two states is negligible, i.e., $F_{\rm NS}(0^+) = F_{\rm SS}(0^+)$. (2) When $0.4088 < J_2 \leq 0.4574$, the free energy curves of the two states cross. The examples are the curves with $J_2 = 0.43$ in Fig. 9(c). At cross point, a first-order phase transformation between NS and SS may occur. Below the cross point, SS is more stable. Above the cross point, NS is more stable. (3) When $J_2 > 0.4574$, $F_{\rm NS}(T)$ is always greater than $F_{\rm SS}(T)$. The examples are the curves in Fig. 8(d). In this case, SS is more stable. Fig. 8 reflects a fact that, as the value of J_2 increases, the value of $F_{\rm NS}(0^+)$ is rising, while $F_{\rm SS}(0^+)$ is decreasing. So on the whole, the curve of $F_{\rm NS}$ is rising, and $F_{\rm SS}$ is down.

Let us make a summary of our results for the case of $J_2 \neq J_{1b}/2$.

(i) The higher the critical temperature, the lower the $F(0^+)$, and the larger the difference between the critical temperature of NS and SS, the larger the difference between $F_{\rm NS}(0^+)$ and $F_{\rm SS}(0^+)$.

(ii) For $J_2 < J_{1b}/2$, $F_{\rm NS}(T)$ is always less than $F_{\rm SS}(T)$, i.e., in this case, NS is always more stable.

(iii) When $J_2 > J_{1b}/2$, one should distinguish three cases. (a) When $J_{1b}/2 < J_2 < J_{2,c1}$, $F_{\rm NS}(T)$ is still less than $F_{\rm SS}(T)$. (b) When $J_{2,c1} < J_2 < J_{2,c2}$, $F_{\rm NS}(0^+)$ becomes greater than $F_{\rm SS}(0^+)$, and the free energy curves of the two states have a cross point, at which a first-order phase transformation between NS and SS may occur. (c) When $J_2 > J_{2,c2}$, $F_{\rm NS}(T)$ is always greater than $F_{\rm SS}(T)$. The $J_{2,c1}$ and $J_{2,c2}$ values depend on the values of η and J_{1b}.

4 Concluding remarks

In this paper, a possible phase transition of the 2D frustrated anisotropic J_{1a}–J_{1b}–J_2 Heisenberg antiferroamgnetic model with spin-1/2 has been studied by means of the double-time Green's function method. Our results have shown that under the condition of $0 \leq \eta < 1$ the NS and SS have the same critical temperature as long as $J_2 = J_{1b}/2$. For the case of $J_2 \neq J_{1b}/2$, our results indicate that these two states can also exist, while they have different critical temperatures. Thus a possible phase transformation between NS and SS with the case of $J_2 = J_{1b}/2$ and $J_2 \neq J_{1b}/2$ has been also discussed, respectively.

In order to discuss explicitly which state is more stable, free energy as a function of temperature is calculated.

When $J_2 = J_{1b}/2$, our results show that the effect of J_{1b} and η on the free energies of the NS and SS may be divided into four regions, see Fig. 8. In region I, the difference between the free energies of the NS and SS is

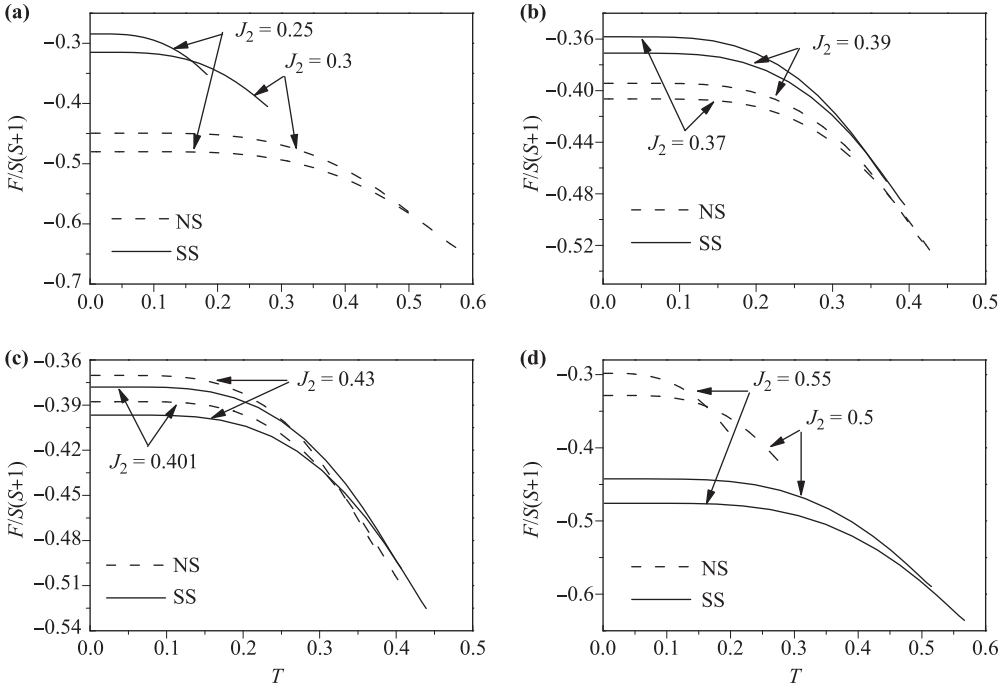

Fig. 9 The free energies $F(T)$ as a function of the temperature T for different J_2 values when $\eta = 0.5$ and $J_{1b} = 0.8$. **(a)** $J_2 = 0.25$, 0.3, **(b)** $J_2 = 0.37$, 0.39, **(c)** $J_2 = 0.401$, 0.43, **(d)** $J_2 = 0.5$, 0.55.

negligible, i.e., $F_{\rm NS} = F_{\rm SS}$. In this case, the system can be in either the NS or SS, a coexistence of them. In region II, $F_{\rm NS} < F_{\rm SS}$, NS is more stable. In region III, a first-order phase transition between NS and SS can occur at a temperature. Below temperature of the cross point, NS is more stable. Above temperature of the cross point, SS is more stable. For region IV, $F_{\rm NS} > F_{\rm SS}$, SS is more stable.

For the case of $J_2 \neq J_{1b}/2$, when $J_2 < J_{1b}/2$, the NS is always more stable than the SS below $T_{\rm N,SS}$. But for $J_2 > J_{1b}/2$, there are three cases. (i) When J_2 takes value in the vicinity of $J_{1b}/2$, the NS is more stable. (ii) When the J_2 value increases further, a first-order phase transformation between the two states may occur. Therefore, in this case, when the temperature approaches zero, the SS is more stable. Near $T_{\rm N,NS}$, the NS is more stable. (iii) When the J_2 value continues increasing, the SS is more stable.

Acknowledgements A. Y. Hu would like to thank Prof. Huai-Yu Wang of Tsinghua University for useful discussions. This work was supported by the National Natural Science Foundation of China (Grant Nos. 11404046 and 11875010) and the Foundation for the Creative Research Groups of Higher Education of Chongqing (No. CXTDX201601016).

References

1. G. Misguich and C. Lhuillier, Frustrated Spin Systems, 2nd Ed., edited by H. T. Diep, World Scientific, 2013
2. J. R. Viana and J. R. deSousa, Anisotropy effects in frustrated Heisenberg antiferromagnets on a square lattice, *Phys. Rev. B* 75(5), 052403 (2007)
3. Y. Z. Ren, N. H. Tong, and X. C. Xie, Cluster mean-field theory study of J_1–J_2 Heisenberg model on a square lattice, *J. Phys.: Condens. Matter* 26(11), 115601 (2014)
4. S. S. Gong, W. Zhu, D. N. Sheng, O. I. Motrunich, and M. P. A. Fisher, Plaquette ordered phase and quantum phase diagram in the spin-1/2 J_1–J_2 Square Heisenberg Model, *Phys. Rev. Lett.* 113(2), 027201 (2014)
5. H. C. Jiang, H. Yao, and L. Balents, Spin liquid ground state of the spin-1/2 square J_1–J_2 Heisenberg model, *Phys. Rev. B* 86(2), 024424 (2012)
6. B. Schmidt, M. Siahatgar, and P. Thalmeier, Ordered moment in the anisotropic and frustrated square lattice Heisenberg model, *Phys. Rev. B* 83(7), 075123 (2011)
7. R. Darradi, O. Derzhko, R. Zinke, J. Schulenburg, S. E. Krüger, and J. Richter, Ground state phases of the spin-1/2 J_1–J_2 Heisenberg antiferromagnet on the square lattice: A high-order coupled cluster treatment, *Phys. Rev. B* 78(21), 214415 (2008)
8. R. L. Doretto, Plaquette valence-bond solid in the square-lattice J_1–J_2 antiferromagnet Heisenberg model: A bond operator approach, *Phys. Rev. B* 89(10), 104415 (2014)
9. T. Roscilde, A. Feiguin, A. L. Chernyshev, S. Liu, and S. Haas, Anisotropy-induced ordering in the quantum J_1–J_2 antiferromagnet, *Phys. Rev. Lett.* 93(1), 017203 (2004)
10. J. F. Yu and Y. J. Kao, Spin-1/2 J_1–J_2 Heisenberg antiferromagnet on a square lattice: A plaquette renormalized tensor network study, *Phys. Rev. B* 85(9), 094407 (2012)
11. R. F. Bishop, P. H. Y. Li, D. J. J. Farnell, and C. E. Campbell, Magnetic order in a spin-1/2 interpolating square-triangle Heisenberg antiferromagnet, *Phys. Rev. B* 79(17), 174405 (2009)
12. R. F. Bishop, P. H. Y. Li, R. Darradi, J. Schulenburg, and J. Richter, Effect of anisotropy on the ground-state magnetic ordering of the spin-half quantum $J_1^{XXZ} - J_2^{XXZ}$ model on the square lattice, *Phys. Rev. B* 78(5), 054412 (2008)
13. L. Wang, Z. C. Gu, F. Verstraete, and X. G. Wen, Tensor-product state approach to spin-12 square J_1–J_2 antiferromagnetic Heisenberg model: Evidence for deconfined quantum criticality, *Phys. Rev. B* 94(7), 075143 (2016)
14. N. D. Mermin and H. Wagner, Absence of ferromagnetism or antiferro-magnetism in one- or two-dimensional isotropic Heisenberg models, *Phys. Rev. Lett.* 17(22), 1133 (1966)
15. A. A. Nersesyan and A. M. Tsvelik, Spinons in more than one dimension: Resonance valence bond state stabilized by frustration, *Phys. Rev. B* 67(2), 024422 (2003)
16. K. Majumdar, Second-order quantum corrections for the frustrated spatially anisotropic spin-1/2 Heisenberg antiferromagnet on a square lattice, *Phys. Rev. B* 82(14), 144407 (2010)
17. K. Majumdar, Magnetic phase diagram of a spatially anisotropic, frustrated spin-1/2 Heisenberg antiferromagnet on a stacked square lattice, *J. Phys.: Condens. Matter* 23(4), 046001 (2011)
18. A. A. Tsirlin and H. Rosner, Extension of the spin-1/2 frustrated square lattice model: The case of layered vanadium phosphates, *Phys. Rev. B* 79(21), 214417 (2009)
19. O. Volkova, I. Morozov, V. Shutov, E. Lapsheva, P. Sindzingre, O. Cépas, M. Yehia, V. Kataev, R. Klingeler, B. Büchner, and A. Vasiliev, Realization of the Nersesyan–Tsvelik model in $(NO)(Cu(NO_3)_3)$, *Phys. Rev. B* 82(5), 054413 (2010)
20. O. Janson, A. A. Tsirlin, and H. Rosner, Antiferromagnetic spin-1/2 chains in $(NO)Cu(NO_3)_3$: A microscopic study, *Phys. Rev. B* 82(18), 184410 (2010)
21. H. Y. Wang, Green's Function in Condensed Matter Physics, Alpha Science International Ltd. and Science Press, 2012
22. P. Fröbrich and P. J. Kuntz, Many-body Green's function theory of Heisenberg films, *Phys. Rep.* 432(5–6), 223 (2006)
23. A. Y. Hu and Q. Wang, The magnetic properties of three-dimensional spin-1 easy-axis single-ion anisotropic antiferromagnets, *Solid State Commun.* 150(13–14), 568 (2010)
24. A. Y. Hu and H. Y. Wang, The exchange interaction values of perovskite-type materials $EuTiO_3$ and $EuZrO_3$, *J. Appl. Phys.* 116(19), 193903 (2014)
25. H. Y. Wang, L. J. Zhai, and M. Qian, The internal energies of Heisenberg magnetic systems, *J. Magn. Magn. Mater.* 354(3), 309 (2014)